Journal of Catalysis **209,** 166–176 (2002)
doi:10.1006/jcat.2002.3625

Bifunctional Metal/Base Catalysts (Pt/X) for the Direct Synthesis of MIBK from Acetone

Lisiane V. Mattos,[*,1] Fábio B. Noronha,[†] and José Luiz F. Monteiro[*,2]

[*] *NUCAT-COPPE-UFRJ, Universidade Federal do Rio de Janeiro, Ilha do Fundão, C.P. 68502, CEP 21945-970 Rio de Janeiro, Brazil; and*
[†] *Instituto Nacional de Tecnologia (INT), Av. Venezuela, 82, CEP 20081-310, Rio de Janeiro, Brazil*

Received December 4, 2001; revised March 19, 2002; accepted March 19, 2002

The synthesis of MIBK was studied over Pt supported on NaX and CsX zeolites. The activity increased as both the temperature and the H_2/Ac ratio were increased. Temperature had also a beneficial effect on the selectivity to MIBK but the H_2/Ac ratio had an opposite effect. Activities and selectivities were always higher for Pt/NaX than for Pt/CsX. For Pt/NaX, increasing the reduction temperature increased the activity but decreased the selectivity to MIBK. Both catalysts were quite stable and selectivities to MIBK of 70% were obtained over PtNaX at 613 K and $H_2/Ac = 0.5$. The absence of both strong acidic and strong basic sites and a proper balance between metallic and basic sites are responsible for the behavior observed. © 2002 Elsevier Science (USA)

Key Words: **acetone; methyl isobutyl ketone; Pt/X zeolites, one-step process.**

INTRODUCTION

Methyl isobutyl ketone (MIBK) is the most important product obtained from acetone (Ac). It is used mainly as a solvent for paints, inks, lacquers, and protective coating systems (1, 2), but it is also used in the extraction of inorganic salts (3) and as a reagent in dewaxing mineral oils (4). It is produced commercially by a three-step process in liquid phase: (i) aldol condensation of acetone to diacetone alcohol (DAA) over basic ($Ba(OH)_2$, NaOH, KOH, and $Ca(OH)_2$) or acidic catalysts; (ii) acid (H_3PO_4, H_2SO_4)-catalyzed DAA dehydration to mesityl oxide (MO); and (iii) selective hydrogenation of MO to MIBK over nickel or copper chromite or over noble metal catalysts (1, 3, 5–7). The two first steps are conventional homogeneous processes and are usually equilibrium limited and the third one may yield a relatively large amount of less useful methyl isobutyl carbinol (MIBC). Furthermore, these processes require many separation and neutralization steps, present corrosion problems, and represent a significant risk to the environment, and the operational costs are high. Those drawbacks strongly induced the search for a one-step process using a catalyst that may perform condensation, dehydration, and reduction simultaneously. Irreversibly hydrogenating MO to MIBK would favorably shift the equilibrium of the other two previous steps. Furthermore, rapid removal of mesityl oxide from the product mixture before it can enter into further condensations prevents the formation of high-boiling products (8).

Several patents can be found on the use of bifunctional catalysts for the one-step synthesis of MIBK in liquid phase using palladium as the active metal (9–16). Various acidic and basic supports have been used, such as KOH–Al_2O_3 (9), MgO–SiO_2 (10), CaO–MgO–SrO–Al_2O_3 (11), Nb_2O_5 (12, 17), $Zr_3(PO_4)_2$ (1, 5), $ZrO(OH)_2$–C (13), Ce, Hf, and/or Ta oxides–C (14), resin (15), C (+ resins) (16), and $Nb_2O_5 + SiO_2$ (18).

When the reaction is carried out in a batch, the rate of reaction decreases very rapidly due to water buildup in the system (17, 18). This limitation can be overcome in a continuous system. In such a case, process conditions often comprise temperatures in the range 393–433 K, pressures between 20–50 bar, and hydrogen/acetone molar ratios of 0.15–0.4, and very stable operation can be achieved (1, 17, 18). Although very high selectivities to MIBK (>90%) at acetone conversions of about 30–40% have been reported, the high operating pressures are a limitation of the liquid-phase single-step process (19).

So, there has recently been a trend for gas-phase single-step processes operating at atmospheric pressure. Reports can be found on the use of Pd supported on SAPO-34 (20), SAPO-11 (6), $AlPO_4$-11 (6), calcined hydrotalcites (21), ZSM-5 (22–25), and Na–MgO (4); of Pt supported on ZSM-5 (7, 25–27); of Ni supported on MgO (19), ALPON (28), Al_2O_3 (29), calcined hydrotalcites (20), and ZSM-5 (30); and of Cu supported on MgO (3). The results show that selectivities to MIBK in gas phase are usually below 80% (although Narayanan and Unnikrishnan (29) have reported values as high as 95%, they did not measure gaseous products), especially due to the parallel hydrogenation of acetone leading ultimately to propene. However, the major limitation seems to be the catalyst stability. Whenever

---

[1] Present Address: Instituto Nacional de Tecnologia (INT), Av. Venezuela, 82, CEP 20081-310, Rio de Janeiro, Brazil.

[2] To whom correspondence should be addressed. Fax: (55-21) 25628300. E-mail: monteiro@peq.coppe.ufrj.br.

0021-9517/02 $35.00

reported, it is always very poor (7, 24–26, 29) over acidic supports, since on these supports coke formation leads to fast deactivation of the catalyst. On mildly acidic or basic supports, reported catalyst stabilities (4, 6, 21) were somewhat better, but still limited. In all of those gas-phase studies, the temperature of reaction was kept below 473 K so as to minimize further condensation reactions leading to the formation of high-boiling point products and catalyst deactivation. The only exception seems to be the work of Chikán *et al.* (3), who reported a reasonable constant MIBK yield over the course of 24 h TOS (conversion decrease was counterbalanced by increasing MIBK selectivity along the run) at 553 K on Cu/MgO catalyst. Trying to suppress the deactivation by increasing the hydrogen/acetone molar ratio increases the hydrogenation of acetone to isopropanol, thus reducing the yield of methyl isobutyl ketone. On the other hand, a too-low hydrogen/acetone ratio not only contributes to catalyst deactivation, it also limits acetone conversion. The production of MIBK requires 1 mol of hydrogen for every 2 mol of acetone (not taking into account the direct hydrogenation of acetone), so that hydrogen is the limiting reactant for hydrogen/acetone ratios below 0.5.

We have previously reported the formation of MIBK over CsX zeolites at 563 K and hydrogen/acetone = 6.2 (molar ratio) (31). Since no data could be found on the one-step synthesis of MIBK from acetone over Pt on mildly basic supports in gas phase, the goal of this work was to study the effect of hydrogen/acetone ratio, reaction temperature, and metal particle size on this reaction over platinum (~1 wt%) supported on X zeolites with Na and Cs as compensating cations. Expectedly, the use of a mildly basic support could overcome the stability limitations mentioned before.

EXPERIMENTAL

Catalyst Preparation

The parent sample was a NaX zeolite (Si/Al = 1.2) obtained from IPT (Instituto de Pesquisas Tecnológicas, São Paulo, Brazil). It was ion exchanged ($Cs^+/Na^+ = 1.5$) with a 0.85 M CsCl solution (sample CsX) and/or with a 5×10^{-3} M $Pt(NH_3)_4Cl_2$ solution to give samples PtCsX and PtNaX, respectively. The solutions were added dropwise under stirring for 6 h to an aqueous suspension with 4 wt% solids at 353 K and kept at room temperature for 20 h. After filtration and washing until no chloride was detected in the filtrate, the samples were dried overnight at 393 K. Next, they were calcined under pure O_2 (1.0 L/g/min) at 1 K/min up to 633 K and kept at the final temperature for 2 h. Then, the calcined samples were reduced under H_2 at 5 K/min up to 633 or 773 K. Three samples were obtained: (i) Pt6/X6 (PtNaX calcined and reduced at 633 K), (ii) Pt7/X6 (PtNaX calcined at 633 K and reduced at 773 K), and (iii) Pt6/CsX6 (PtCsX calcined and reduced at 633 K).

Catalyst Characterization

A detailed description of the characterization of the present catalysts is beyond the scope of this work and will be given in another paper, under preparation. The information given here is that necessary for the proper interpretation of the catalytic results.

The chemical composition was determined by atomic absorption (Na, Pt, Si, and Al) and atomic emission (Cs) spectrometry on a Perkin–Elmer AAS 1100B spectrophotometer. ^{29}Si-, ^{27}Al-, and ^{133}Cs-MAS–NMR spectra were recorded on a Bruker DRX-300 spectrometer with a 7-mm zirconia rotor spun at 5 kHz for Si and Al and at 14 kHz for Cs. Spectra were taken at 59.6 MHz for Si, 78.2 MHz for Al, and 39.4 MHz for Cs. BET specific surface areas and micro- (t-plot) and mesopore (BJH) volumes were determined by N_2 adsorption at 77 K on a Micromeritics ASAP 2000. The crystallinity of the samples was determined by XRD using a Rigaku Dmax Ultima$^+$ diffractometer with Cu$K\alpha$ radiation, 40 kV and 40 mA.

H_2 chemisorption (Micromeritics ASAP 2900 C) and transmission electronic microscopy (JEOL 2010 microscope) were used to determine metal particle size and dispersion. For TEM analyses, sections with thickness around 80–90 nm were obtained with a microtome. The particle size as given by TEM was taken from various micrographs. About 700 particles were examined for each sample and the average diameter, assuming spherical particles, was determined from (32)

$$d = \frac{\sum n_i \times d_i^3}{\sum n_i \times d_i^2}, \qquad [1]$$

where n_i is the number of particles with diameter d_i.

Dispersions and particle sizes were related by (33)

$$d = \frac{1}{D}. \qquad [2]$$

IR spectra were recorded with a Perkin–Elmer FTIR 2000 spectrophotometer at room temperature. Self-supported wafers were used to investigate surface hydroxyls after drying at 633 K for 2 h under He and evacuation at 10^{-4} Torr for 1 h at this same temperature. Acid sites were probed by pyridine adsorption at 423 K followed by evacuation at 10^{-4} Torr for 30 min at this temperature. All spectra were taken at room temperature.

Reaction Conditions

The gas-phase reaction was carried out in a fixed-bed reactor at atmospheric pressure. Various independent runs at different temperatures, space velocities, and H_2/Ac molar ratios were performed. The reactants were fed to the reactor by bubbling hydrogen through a saturator held at the desired temperature. The exit stream was analyzed by online gas chromatography with a Carbowax 20 M column and a flame ionization detector.

The conversion of acetone (X_A) and the selectivity (S) to the various products were defined on the basis of converted acetone (5, 8).

$$X_A = \frac{y_M + 2 \times y_D + 3 \times y_T}{y_A + y_M + 2 \times y_D + 3 \times y_T}, \quad [3]$$

$$S = \frac{y_M, 2 \times y_D \text{ or } 3 \times y_T}{y_M + 2 \times y_D + 3 \times y_T}, \quad [4]$$

where y_A, y_M, y_D, and y_T are, respectively, the mole fractions of acetone, monomers (IPA, C3), dimers (DAA, IMO, MO, MIBK, MIBC), and trimers (DIBK, DMHA) in the product stream.

Accordingly, the activities were also defined on the basis of converted acetone (mol Ac/h/g_{cat}), as follows.

$$\text{Overall activity, } A_o = \frac{X_A \times \text{WHSV}}{58}. \quad [5]$$

$$\text{Activity for acetone hydrogenation, } A_h = A_o \times S_M. \quad [6]$$

$$\text{Activity for acetone condensation, } A_c = A_o \times (S_D + S_T). \quad [7]$$

Conversion, selectivity, and activity values reported for each run refer to those taken at steady conditions, typically at 180 min TOS.

RESULTS

Characteristics of the Samples

The unit cells of the calcined samples were $Pt_{0.62}Na_{83.8}Al_{85}Si_{107}O_{384}$ (0.90 wt% Pt) and $Pt_{0.91}Cs_{42.2}Na_{41}Al_{85}Si_{107}O_{384}$ (0.98 wt% Pt). ^{29}Si-MAS–NMR gave SAR (silica/alumina ratio) values of 2.3–2.4 for all the calcined and reduced samples used in this work, a value very close to that of the bulk composition (2.4).

Absence of extraframework aluminum species was confirmed by ^{27}Al-MAS–NMR. A signal at 31 ppm in the ^{133}Cs-MAS–NMR spectrum of the cesium-containing sample after calcination is due to Cs cations in the zeolite cavities (34).

Various TPD–, TPR–, and TPO–MS experiments showed no signals that could be attributed to chlorine species. The same applies to XPS and XRF analyses.

All samples exhibited type I isotherms, characteristic of microporous materials. No mesopores were observed. The BET areas and the micropore volumes were not affected by the various treatments (Table 1). For the sodium sample those values were within the range 650–660 m^2/g and 0.30–0.31 cm^3/g, respectively. For the cesium samples the corresponding values were 450–490 m^2/g and 0.20–0.22 cm^3/g, since the bulky cesium cations limit the space available within the cavities.

TABLE 1

BET Areas and Micropore Volumes as Determined by N_2 Adsorption

Sample	BET area (m^2/g)	Micropore volume (cm^3/g)
NaX	656	0.30
CsX	490	0.22
Pt6/X6	660	0.30
Pt7/X6	650	0.31
Pt6/CsX6	450	0.20

XRD analyses confirmed that the crystallinity of the samples was preserved along the various treatments.

The results obtained from H_2 chemisorption and TEM are shown in Table 2. The particle size distribution for samples Pt6/X6 and Pt7/X6 are presented in Fig. 1. The metal particle size was not significantly affected by the nature of the compensating cation but the particles became larger when the temperature of reduction was increased from 633 to 773 K.

Most of the particles were located within the zeolite crystal, most probably causing a local disruption of the framework, small enough not to be detected by the textural analysis. Although only a relatively small fraction of the metal particles (the largest ones, between 3.0 and 5.0 nm) were on the external surface, particularly for the sample reduced at the lower temperature, they contributed heavily to the overall dispersion and average particle size.

Figure 2 shows the results obtained from infrared analyses in the hydroxyl region. For both samples NaX and PtNaX after calcination only a band around 3690 cm^{-1} was observed, which is attributed to the interaction of water with the sodium cation (35). This band was not observed for sample CsX, since the interaction of this cation with water is much weaker (36). No bands associated to hydroxyl groups could be seen either before or after the ion-exchange and calcination steps, confirming the absence of structural defects and of bridged hydroxyls.

The IR results for sample Pt6/X6 obtained after pyridine adsorption are presented in Fig. 3. The band related to Brønsted acid sites could hardly be seen at 1540 cm^{-1}, indicating that even the reduced samples had a very small

TABLE 2

Dispersion (*D*) and Average Particle Size (*d*) as Given by H_2 Chemisorption and TEM

	H_2 chemisorption		TEM	
Sample	*D* (%)	*d* (nm)	*d* (nm)	*D* (%)
Pt6/X6	35	2.8	3.1	32
Pt7/X6	25	4.0	3.7	27
Pt6/CsX6	30	3.3	2.5	40

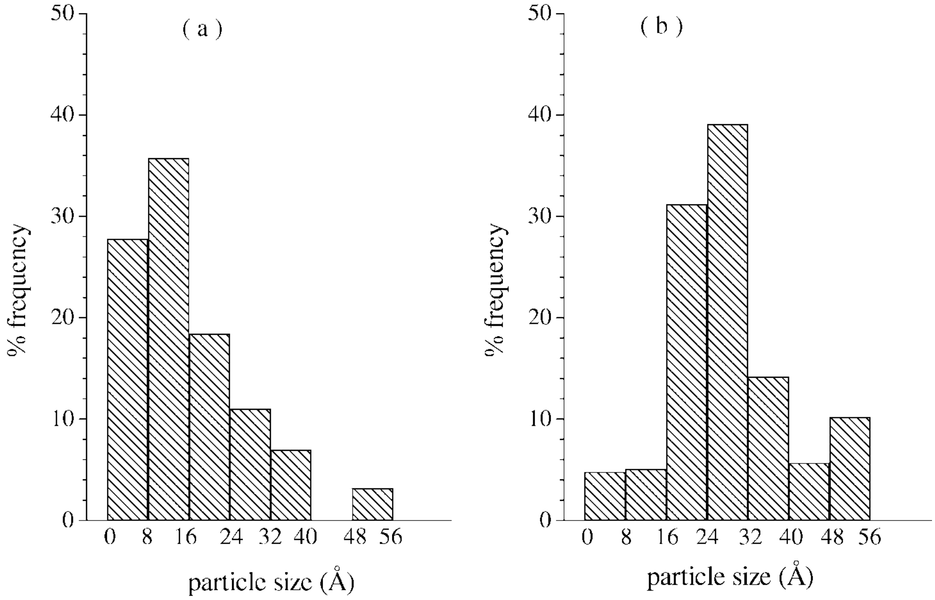

FIG. 1. Particle size distribution as determined from TEM micrographs for samples calcined at 633 K and reduced at (a) 633 K (sample Pt6/X6) and (b) 773 K (sample Pt7/X6).

Brønsted acidity. Only bands due to the interaction of pyridine with the cations could be detected at 1439 and 1484 cm^{-1}.

Reaction Products

The products resulting from acetone (Ac) transformation over all the samples were propane (C3), isopropyl alcohol (IPA), methyl isobutyl ketone (MIBK), methyl isobutyl carbinol (MIBC), diisobutyl ketone (DIBK), and 2,6-dimethyl-2-hepten-4-ol (DMHA). Formation of these products can be explained by means of the following reaction scheme (Fig. 4). DAA formed by the aldol condensation of acetone on basic sites is dehydrated to mesityl oxide (MO) and its isomer (IMO), which are hydrogenated to MIBK on metallic sites. MIBK may go through additional condensation and hydrogenation steps, ultimately leading to DIBK and DMHA, or it may be hydrogenated to MIBC. Along a parallel reaction, acetone can also be directly hydrogenated to IPA, which is dehydrated and hydrogenated to propane. Therefore, acetone transformation occurred by two main routes: (i) hydrogenation of acetone,

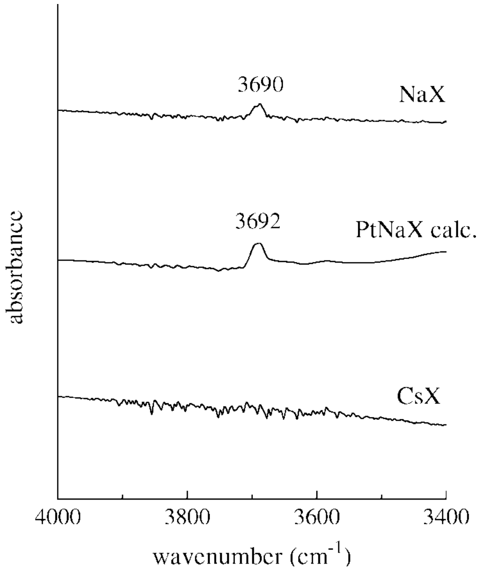

FIG. 2. Infrared spectra for samples NaX, PtNaX (after calcination), and CsX in the hydroxyl region.

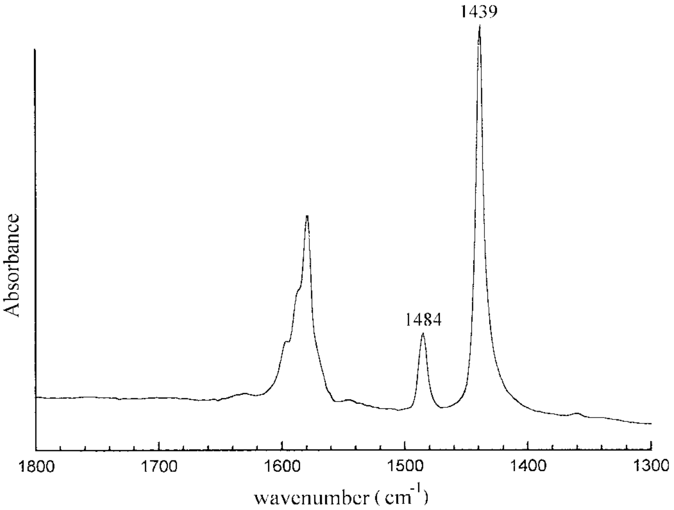

FIG. 3. Infrared spectrum of adsorbed pyridine for the sample calcined and reduced at 633 K (sample Pt6/X6).

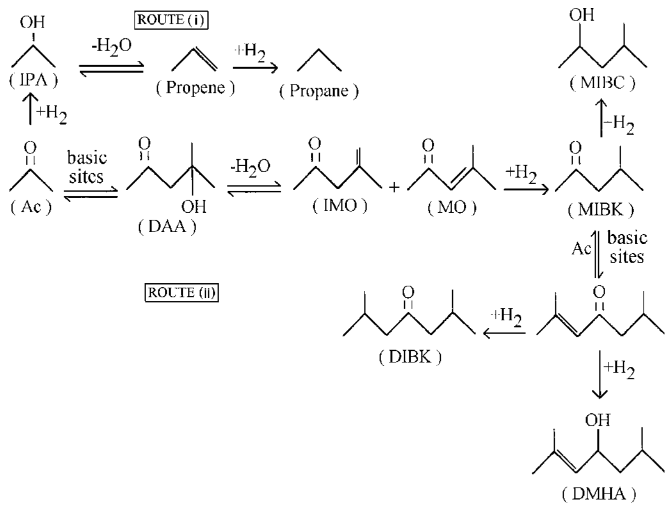

FIG. 4. Main reactions observed during acetone transformation.

TABLE 3

Effect of H_2/Ac Ratio on the Overall Activity (A_o), on the Activity for Acetone Hydrogenation (A_h), and on the Activity for Aldol Condensation of Acetone (A_c) ($T = 563$ K)

Sample	H_2/Ac (molar ratio)	WHSV (h^{-1})	X_A (%)	A_o (mol/h/g_{cat})	A_h (mol/h/g_{cat})	A_c (mol/h/g_{cat})
Pt6/X6	0.5	106	6.7	0.12	0.045	0.076
Pt6/X6	6.2	295	9.3	0.47	0.415	0.055
Pt6/CsX6	0.5	27	7.4	0.035	0.017	0.018
Pt6/CsX6	6.2	50	7.8	0.070	0.059	0.011

producing IPA and C3, and (ii) aldol condensation of acetone, forming MIBK and other condensation products. DAA, MO, IMO, propene, isobutene, and heavier compounds (phorone, isophorone, isoxylitones, etc.) were not observed among the products.

Effect of H_2/Ac Ratio

For both samples reduced at 633 K, increasing the H_2/Ac ratio at nearly isoconversion at 563 K had a positive effect on the overall activity (Table 3), since the direct hydrogenation of acetone increased significantly. However, the activity for the aldol condensation reaction slightly decreased. As a consequence, the selectivity to MIBK (Fig. 5) was significantly reduced, particularly for the sample in the sodium form. The same was observed for the selectivities to DIBK and DMHA. On the other hand, MIBC production was not favored. Moreover, the results (Fig. 5) show that increasing the H_2/Ac ratio decreased the C3/IPA ratio, and that the selectivity to both of them increased.

Effect of Reaction Temperature

Taking into account the results reported in the previous section, the influence of temperature was studied at H_2/Ac = 0.5 for the samples reduced at 633 K.

Now, for the sample in the sodium form, increasing the reaction temperature from 563 to 613 K at a conversion of about 10% increased both the overall activity and the activity for aldol condensation of acetone, but decreased its rate of hydrogenation (Table 4). For the sample in the cesium form, this behavior held for the overall and for the condensation activity as the temperature was raised, but now also the hydrogenation activity showed a slight increasing trend. For this sample, very limited activity for condensation was observed below 473 K, a range of temperatures usually employed when acid catalysts are used.

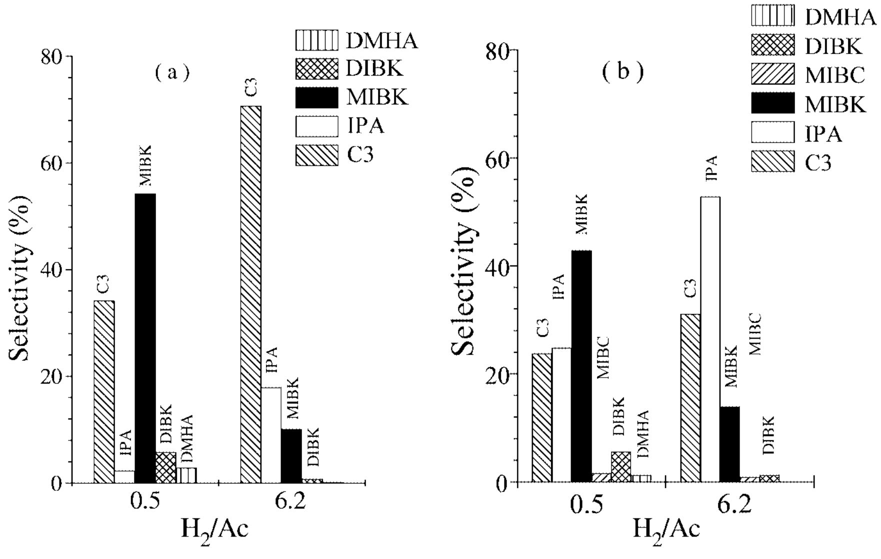

FIG. 5. Effect of H_2/Ac molar ratio on the selectivity at 563 K: (a) Pt6/X6 and (b) Pt6/CsX6.

TABLE 4

Effect of Reaction Temperature on the Overall Activity (A_o), on the Activity for Acetone Hydrogenation (A_h), and on the Activity for Aldol Condensation of Acetone (A_c) (H_2/Ac = 0.5)

Sample	T (K)	WHSV (h^{-1})	X_A (%)	A_o (mol/h/g_{cat})	A_h (mol/h/g_{cat})	A_c (mol/h/g_{cat})
Pt6/X6	563	106	6.7	0.120	0.045	0.076
Pt6/X6	613	154	7.2	0.190	0.029	0.161
Pt6/CsX6	413	6	12.6	0.013	0.013	2.26×10^{-4}
Pt6/CsX6	473	13.5	13.0	0.030	0.025	0.005
Pt6/CsX6	563	27	7.4	0.035	0.017	0.018
Pt6/CsX6	613	54	8.3	0.076	0.025	0.051

TABLE 5

Effect of Reduction Temperature (T_{red}) on the Overall Activity (A_o), on the Activity for Acetone Hydrogenation (A_h), and on the Activity for Aldol Condensation of Acetone (A_c) for Sample PtNaX Calcined at 633 K (H_2/Ac = 0.5)

Sample	T_{red} (K)	T (K)	WHSV (h^{-1})	X_A (%)	A_o (mol/h/g_{cat})	A_h (mol/h/g_{cat})	A_c (mol/h/g_{cat})
Pt6/X6	633	563	106	6.7	0.12	0.045	0.076
Pt7/X6	773	563	159	6.7	0.18	0.108	0.072
Pt6/X6	633	613	181	5.6	0.17	0.023	0.147
Pt7/X6	773	613	242	5.0	0.21	0.042	0.168

Also, for both samples the increase in the reaction temperature favored the dehydration of IPA (Fig. 6). This had a positive effect on C3 selectivity for sample Pt6/CsX6 but not for sample Pt6/X6, since for the latter the enhanced dehydration of IPA did not overcome the reduction of the activity along the hydrogenation route when the temperature was increased. Only trace amounts of C3 were observed at or below 473 K.

The selectivity to MIBK was also favored by higher temperatures. As a consequence, large selectivities to MIBK (≅70%) were obtained over Pt6/X6 at 613 K and H_2/Ac = 0.5, since at this temperature the hydrogenation of acetone to IPA was largely inhibited. However, further transformation of MIBK also took place, thus reducing the MIBK/(MIBC + DIBK + DMHA) ratio from 6 to 4 for Pt6/X6 and from 5 to 3 for Pt6/CsX6.

Effect of Reduction Temperature

The influence of metal dispersion was explored for the sample in the sodium form at H_2/Ac = 0.5.

Whatever the reaction temperature (T), the overall rate of reaction increased when the metal was reduced at a higher temperature (Table 5). A closer look at Table 5 shows that indeed at each reaction temperature the activity for aldol condensation was hardly affected. On the other hand, the rate of acetone hydrogenation over the sample reduced at 773 K is about twice as large as that over the sample reduced at 633 K, for both temperatures of reaction.

The selectivities to the various products was affected in an analogous manner. The selectivity to those formed along the route of acetone hydrogenation (IPA and C3) was larger for the sample reduced at 773 K, while those originating from acetone condensation (MIBK, MIBC, DIBK, DMHA) were selectively obtained over sample Pt6/X6 (Fig. 7).

Effect of the Compensating Cation

For all reaction conditions, the introduction of cesium decreased the overall activity, as can be seen from the data in Tables 3 and 4. The activity for acetone hydrogenation

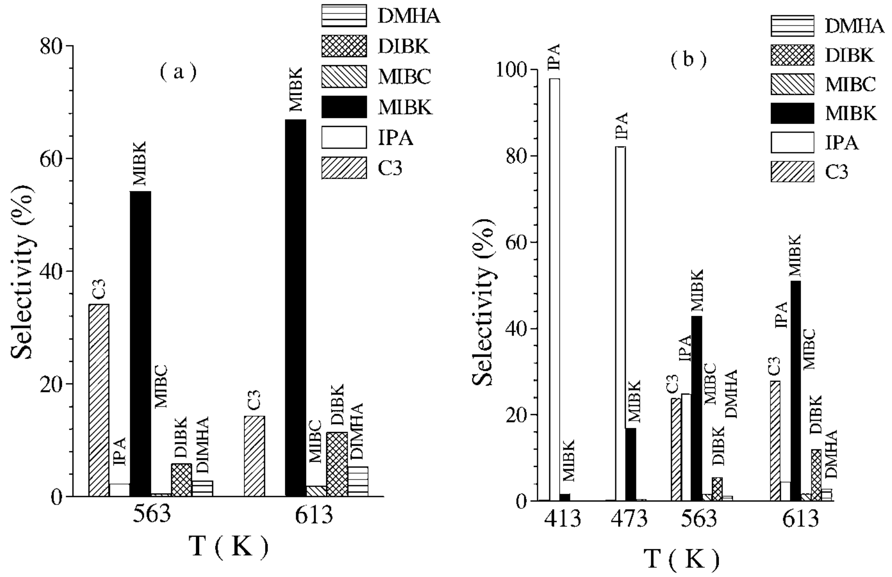

FIG. 6. Effect of reaction temperature on the selectivity for H_2/Ac = 0.5: (a) Pt6/X6 and (b) Pt6/CsX6.

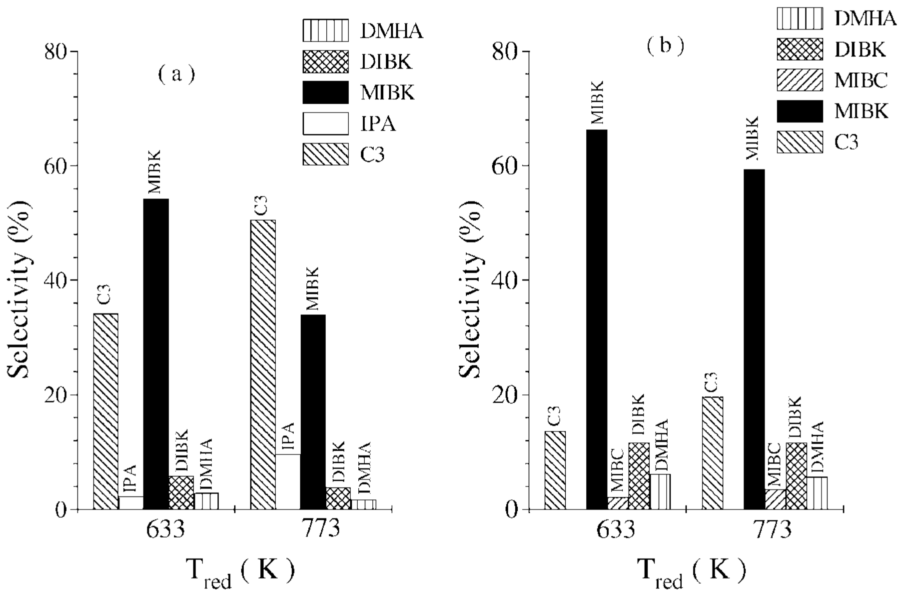

FIG. 7. Effect of reduction temperature on the selectivity over Pt6/X6 and Pt7/X6 for $H_2/Ac = 0.5$: (a) reaction temperature = 563 K and (b) reaction temperature = 613 K.

of the Cs-containing sample was less sensitive to hydrogen partial pressure than that of the sample in the sodium form (Table 3), and it was less affected by increasing reaction temperatures (Table 4). It was also observed that the dehydration reactions were more significant over Pt6/X6 than over Pt6/CsX6 (Fig. 5); as a consequence, C3/IPA ratios were larger over the former (Fig. 5). Moreover, selectivities to MIBK were always smaller over Pt6/CsX6 compared to Pt6/X6.

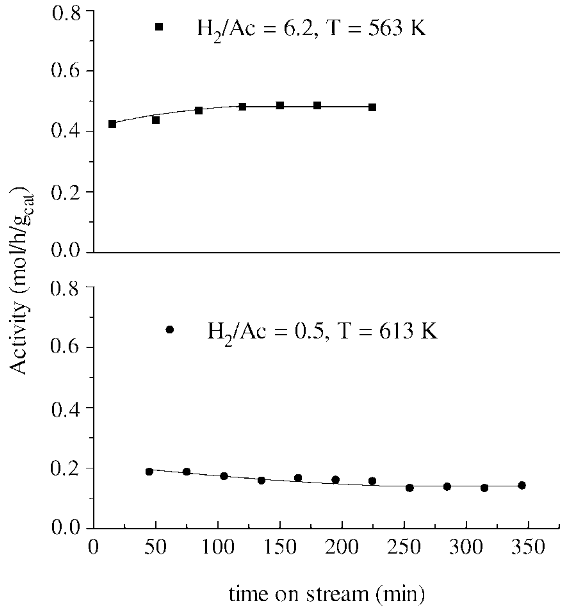

FIG. 8. Activity as a function of time on stream for sample Pt6/X6.

Stability

The stability of sample Pt6/X6 was evaluated at two different conditions and the catalyst was rather stable in both conditions after a small initial transient period. Figure 8 shows the results obtained. When the reaction was run at 563 K and $H_2/Ac = 6.2$, the overall activity increased along the first 120 min on stream, essentially due to an increase in the hydrogenation activity, as can be observed from the selectivity results in Fig. 9. At 613 K and $H_2/Ac = 0.5$, a slight decrease in the activity was observed in the beginning of the run, but the catalyst became quite stable after about 180 min time on stream (TOS). On the other hand the

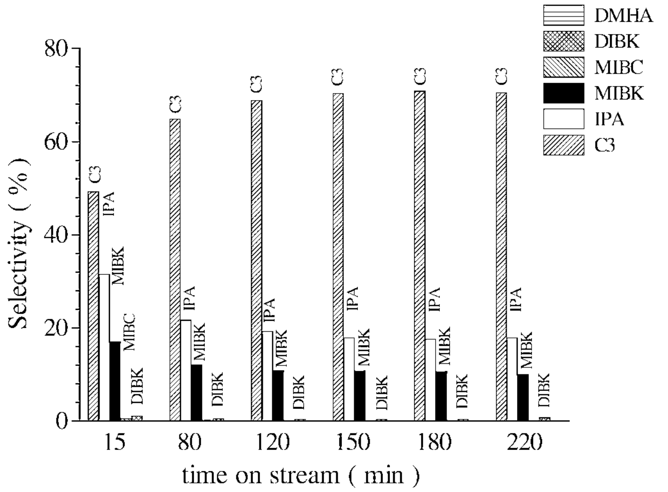

FIG. 9. Selectivity as a function of time on stream ($H_2/Ac = 6.2$, reaction temperature = 563 K).

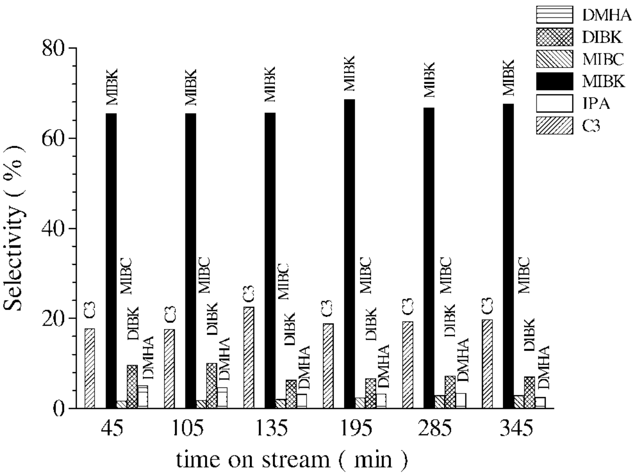

FIG. 10. Selectivity as a function of time on stream (H_2/Ac = 0.5, reaction temperature = 613 K).

selectivities to the various products remained quite constant along the run, as can be seen from Fig. 10.

DISCUSSION

Bifunctional metal/acid catalysts are used in a variety of commercial processes, especially in refining and petrochemicals production, such as reforming, hydrocracking, hydroisomerization of parafins, and isomerization of aromatics. Bifunctional catalysts usually work under milder conditions than monofunctional ones, their deactivation is much slower and they can perform several steps simultaneously (37). On the other hand, metal catalysts on nonacidic supports have recently attracted much attention, particularly since Pt/KL zeolite catalysts have been shown to be very active and selective for the aromatization of *n*-hexane (38).

Bifunctional catalysts have also a large potential of application in the field of intermediates and fine chemicals, since in these cases a number of successive steps are usually involved. Such is the case for MIBK production, as illustrated in Fig. 4. Actually, many other side reactions and reversible steps could have been drawn (6, 7, 26, 31); their relative contributions to the overall product distribution depend on the catalyst and operational conditions.

The absence of DAA in the present work showed the facility of dehydration of this tertiary alcohol. On the other hand, the absence of mesityl oxides and propene and the presence of MIBC, DIBK, and DMHA is evidence of the hydrogenating capacity of the catalysts studied, particularly for the C=C double bond. The absence of heavier products, contrary to what has been reported by other authors who used basic supports (3, 4, 21), may be related to both a proper balance between the metallic and the basic functions of our catalysts and the steric restraints imposed by the channel system of the zeolite.

Contrary to what is observed on acid catalysts (7, 26), the hydrogenation of acetone was not the controlling step along route (i), since both IPA and C3 were detected in most cases (Figs. 5–7). Similar results have been observed over other basic supports (3, 4, 21). The results in Fig. 5 confirm that the dehydration of IPA was slower than the hydrogenation of acetone since the C3/IPA ratio decreased as the H_2/Ac ratio was increased, at 563 K. IPA dehydration was rapid enough only at 613 K over Pt6/X6 (Figs. 6 and 7). This reaction was always more important over Pt6/X6 than over Pt6/CsX6. This is probably due to the fact that Na^+ cations are stronger Lewis acidic sites than are Cs^+ cations. Although the protons derived from the reduction of Pt^{2+} cations may have contributed to this dehydration, the role of the compensating cation and the absence of C3 at or below 473 K suggests that this effect, if present, was not significant.

The effect of temperature on the activity for the two routes (Table 4) clearly indicates that the activation energy of the condensation reaction is higher than that of acetone hydrogenation, as also observed by Yang and Wu (6) and Chen *et al.* (21). The results from Table 4 show that reducing the metal at a higher temperature increased the hydrogenating activity but not the activity for aldol condensation, thus indicating that the condensation of two molecules of acetone over basic sites is the limiting step of MIBK production along route (ii). This suggests that the amount of platinum used (1.0 wt%) may be reduced, since mesityl oxide hydrogenation proceeded readily over this catalyst. Other metals, like Pd, which has a relatively low activity for C=O hydrogenation, and other basic zeolites should also be tested. The facile hydrogenation of the double bond of the mesityl oxide molecule has been observed over various metals on different supports (18, 26, 30).

The aldol condensation of two molecules of acetone over a solid base can be represented by the following steps (39, 40).

Step A: H^+ abstraction from acetone by the base, forming an enolate anion.

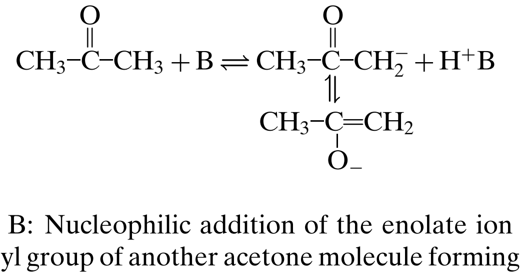

$$\begin{array}{c} CH_3-\overset{\overset{\displaystyle O}{\|}}{C}-CH_3 + B \rightleftharpoons CH_3-\overset{\overset{\displaystyle O}{\|}}{C}-CH_2^- + H^+B \\ \hspace{1.5em}\Updownarrow \\ \hspace{1.5em} CH_3-\underset{\underset{\displaystyle O_-}{|}}{C}=CH_2 \end{array}$$

Step B: Nucleophilic addition of the enolate ion to the carbonyl group of another acetone molecule forming a new C–C bond and an alkoxide ion.

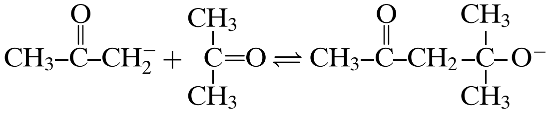

$$CH_3-\overset{\overset{\displaystyle O}{\|}}{C}-CH_2^- + \underset{\underset{\displaystyle CH_3}{|}}{\overset{\overset{\displaystyle CH_3}{|}}{C}}=O \rightleftharpoons CH_3-\overset{\overset{\displaystyle O}{\|}}{C}-CH_2-\underset{\underset{\displaystyle CH_3}{|}}{\overset{\overset{\displaystyle CH_3}{|}}{C}}-O^-$$

Step C: Reaction of the alkoxide ion with H^+ to give diacetone alcohol (DAA).

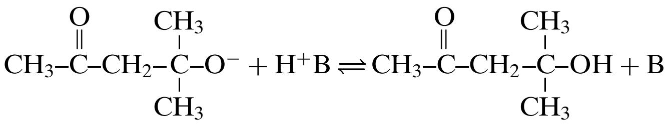

$$CH_3-\overset{O}{\overset{\|}{C}}-CH_2-\underset{CH_3}{\overset{CH_3}{C}}-O^- + H^+B \rightleftharpoons CH_3-\overset{O}{\overset{\|}{C}}-CH_2-\underset{CH_3}{\overset{CH_3}{C}}-OH + B$$

In the case of zeolites the basic sites are the oxygen atoms of the framework.

Since all of those steps are reversible, as is the dehydration of DAA to MO (8), good yields of MIBK can only be attained if hydrogenation of MO proceeds at a rate sufficient enough to shift the equilibrium of the previous steps. This hydrogenation activity should also be selective for the C=C double bond, since the hydrogenation of the carbonyl group of either acetone or MIBK is undesirable.

Our results (Table 5) show that acetone hydrogenation was more intense over the sample reduced at 773 K (Pt7/X6).

Characterization of samples Pt6/X6 and Pt7/X6 by H_2 chemisorption and TEM (Table 2) indicated that the metal particles were larger for the sample reduced at the higher temperature. For this sample, most particles had a size of about 1.6–4.0 nm and many of them were on the outer surface, thus having a limited interaction with the basic sites, mostly located within the channels. The reverse was true for sample Pt6/X6, for which most particles had diameters between 0.0 and 2.4 nm and were located in the porous structure, close to the basic sites.

Yang and Wu (6) and Gandía *et al.* (28) suggested that significant yields of MIBK depend on an adequate balance between basic and metallic sites. In the present work, acetone hydrogenation was favored when the number of metallic particles on the outer surface was large (sample reduced at 773 K) and the ratio between metallic and basic sites was also large. On the other hand, a proper balance between those two types of sites led to a larger selectivity to MIBK when the sample was reduced at 633 K and most metallic particles remained in the zeolite porous system.

When samples Pt6/X6 and Pt6/CsX6 are compared (Tables 3 and 4), both the hydrogenation activity and the condensation activity are lower for the Cs-containing sample. Since this sample is more basic, the decreased condensation activity can be related to the geometric constraints imposed by the bulky cesium cations. As the size and location of the metal particles were similar in both samples, this same reasoning can be used to explain the decreased hydrogenation activity of Pt6/CsX6. However, in this case, an electronic effect may also have played a role, since the particles supported on the more basic cesium-containing sample should be more electron rich.

Finally, the good stability of the samples used in this work can be related to the proper basicity of the supports used. A too-basic support induces additional condensation reactions, creating the heavier products responsible for catalyst deactivation (3, 4). An additional benefit of mildly basic supports is the possibility of using higher temperatures of reaction, thus favoring the desorption of undesirable intermediates like trimers, eventually formed in small amounts, and thus avoiding their further condensation. The desorption of products is also favored from the large pores of zeolite X.

When acidic zeolites are chosen, neither large pore structures nor high temperatures can be used, since coke formation is very rapid. Although HMFI has been suggested (25) and extensively used for this reaction, its stability is also very poor, even when its acidity is reduced (27).

Alkali-exchanged X zeolites have been known for a long time as mildly basic materials (41). Our samples had no significant concentration either of strong basic sites (as further supported by the absence of products derived from Michael condensation reactions such as isophorone) or of strong acidic sites (as shown by IR, by their limited activity for IPA dehydration, and by the absence of isobutene among the reaction products).

In this work, very good selectivities to MIBK (~70%) were obtained over the catalyst calcined and reduced at 633 K, when the reaction was carried out at 613 K and $H_2/Ac = 0.5$ (molar ratio). Since selectivities were defined on the basis of molecules of acetone consumed and the main by-product (C3) is gaseous, the corresponding molar fraction of MIBK in the liquid product is about 0.85. Furthermore, this high selectivity was obtained under conditions for which the catalyst activity was about 0.19 mol $Ac/h/g_{cat}$, which gives a yield of MIBK of 66×10^{-3} $mol/h/g_{cat}$.

When this reaction is performed in one step in liquid phase over Pd supported on basic carriers, the yield of MIBK is impractical (5). When Pd supported on solid acids was used (1, 5, 17, 18), stable continuous operation in liquid phase has been reported with MIBK selectivities above 90%, but the pressures used were rather high. The reported activities ranged between about 4×10^{-3} (17) and 60×10^{-3} (1) mol $Ac/h/g_{cat}$. On the other hand, when the reaction was carried out in gas phase over acidic supports, either the activities were in the lower end of the range mentioned before or the stability was very poor. Most often, both effects were observed. Over basic supports in gas phase (3, 4, 6, 19, 21, 28), activities and stabilities are usually superior to those over acidic supports. Chen *et al.* (21) reported surprisingly high activities over Pd supported on calcined hydrotalcites at 413 K (3.2 mol $Ac/h/g_{cat}$), but the simultaneous formation of heavier products led to limited stability. Chikán *et al.* (3) reported quite stable MIBK yields for 24 h over Cu/MgO catalysts at 553 K, but the activity of their catalyst was relatively low. Although they did not disclose appropriately their experimental conditions, apparently both results derive from the use of diluted (with He) feeds.

Lin and Ko (4) observed an activity of about 0.10 mol Ac/h/g_{cat} and reasonably stable MIBK yield for 8 h TOS over Pd supported on magnesium oxide doped with sodium. The Ni/MgO catalyst of Gandía and Montes (19) showed very little stability while no data are reported on the deactivation of the Ni/ALPON used by Gandía *et al.* (28). All of those basic supports are very strong and this often resulted in good activity but poor stability. To the best of our knowledge, the present work is the first one to use Pt over a basic support and, particularly, to use a basic zeolite as support. The resulting balance between the metallic and the basic functions led to very good MIBK yields and catalyst stability.

CONCLUSIONS

When a direct route for MIBK synthesis from acetone is sought, issues such as activity, selectivity, and stability must be taken into account. Those factors depend on the metal properties (nature, amount, dispersion, localization, and geometric and electronic properties), on the support properties (acid/base character, pore structure, and interactions with the metal), and on the operational conditions (phase, temperature, space velocity, pressure, concentration of reactants, and type of reactor). Liquid-phase heterogeneous one-step processes are very attractive as to selectivity and stability, but the activities are not particularly high and operational costs are a drawback. Gas-phase one-step processes over metallic/acidic catalysts, although extensively studied, have always shown limited activity and poor stability. In those cases when the hydrogenating metal was supported on a basic carrier, some of the results previously reported indicated that fine tuning of the bifunctional catalyst could lead to a gas-phase process economically attractive.

The results obtained in this work show that a Pt/NaX catalyst reduced at 633 K can perform the one-step synthesis of MIBK in gas phase at atmospheric pressure with good activity, selectivity, and stability at 613 K and H_2/Ac molar ratio of 0.5. The absence of both strong acidic and strong basic sites and a proper balance between the metallic and the base functions seem to be responsible for the observed behavior, although requiring a temperature of reaction higher than that usually employed in previous studies. On the other hand, the use of such a temperature was possible only because the basicity of the catalyst was low enough not to promote consecutive condensation reactions that would form heavy products which cause deactivation. Acetone hydrogenation was not the rate-determining step along the route that ultimately leads to propane, contrary to what is observed with acidic catalysts, while the aldol condensation of two molecules of acetone was the limiting step for MIBK production.

ACKNOWLEDGMENTS

We are grateful to Dr. João Poço (IPT—Instituto de Pesquisas Tecnológicas, São Paulo, Brazil) for the NaX zeolite supplied and to IRC (Institut de Recherches sur la Catalyse/France) for TEM analyses. One of the authors (Lisiane V. Mattos) acknowledges the scholarship received from CNPq.

REFERENCES

1. Onoue, Y., Mizutani, Y., Akiyama, S., Izumi, Y., and Watanabe, Y., CHEMTECH 36 (1977).
2. Reith, W., Dettmer, M., Widdecke, H., and Fleischer, B., *Stud. Surf. Sci. Catal.* **59**, 487 (1991).
3. Chikán, V., Molnár, A., and Balázsik, K., *J. Catal.* **184**, 134 (1999).
4. Lin, K. H., and Ko, A. N., *Appl. Catal. A* **147**, L259 (1996).
5. Watanabe, Y., Matsumura, Y., Izumi, Y., and Mizutani, Y., *Bull. Chem. Soc. Jpn.* **47**, 2922 (1974); *J. Catal.* **40**, 76 (1975).
6. Yang, S. M., and Wu, Y. M., *Appl. Catal. A* **192**, 211 (2000).
7. Melo, L., Giannetto, G., Alvarez, F., Magnoux, P., and Guisnet, M., *Catal. Lett.* **44**, 201 (1997).
8. Pittman, C. U., Jr., and Liang, Y. F., *J. Org. Chem.* **45**, 5048 (1980).
9. Smith, E. F., and Haute, T., U.S. Patent 2,499,172 (1950).
10. Distillers, Co., Br. Patent 1,015,003 (1965).
11. Too, Y., and Nakayama, T., Jpn. Patent 62,258,335 (1987).
12. Maki, T., Yokoyama, T., and Sumino, Y., Jpn. Patent 63,68,538 (1988).
13. Maki, T., Yokoyama, T., and Sumino, Y., Jpn. Patent 63,96,147 (1988).
14. Maki, T., Yokoyama, T., and Sumino, Y., Jpn. Patent 63,96,146 (1988).
15. Schmitt, K., Distedorf, J., and Flakus, W., U.S. Patent 3,953,517 (1976).
16. Wollner, J., and Moers, K. K., U.S. Patent 3,405,178 (1968).
17. Higashio, Y., and Nakayama, T., *Catal. Today* **28**, 127 (1996).
18. Chen, Y. Z., Liaw, B. J., Tan, H. R., and Shen, K. L., *Appl. Catal. A* **205**, 61 (2001).
19. Gandía, L. M., and Montes, M., *Appl. Catal. A* **101**, L1 (1993).
20. Olson, K. D., U.S. Patent 4,704,478 (1987).
21. Chen, Y. Z., Hwang, C. M., and Liaw, C. W., *Appl. Catal. A* **169**, 207 (1998).
22. Chen, P. Y., Chu, S. J., Chen, C. C., Chang, N. S., Lin, W. C., and Chuang, T. K., U.S. Patent 5,059,724 (1991).
23. Huang, T. J., and Haag, W. O., U.S. Patent 4,339,606 (1982).
24. Chen, P. Y., Chu, S. J., Lin, W. C., Wu, K. C., and Yang, C. L., *Stud. Surf. Sci. Catal.* **83**, 481 (1994).
25. Magnoux, P., Lavaud, N., Melo, L., Giannetto, G., Silva, A. I., Alvarez, F., and Guisnet, M., *Stud. Surf. Sci. Catal.* **130**, 3011 (2000).
26. Melo, L., Magnoux, P., Giannetto, G., Alvarez, F., and Guisnet, M., *J. Mol. Catal.* **124**, 155 (1997).
27. Melo, L., Giannetto, G., Cardozo, L., Llanos, A., García, L., Magnoux, P., Guisnet, M., and Alvarez, F., *Catal. Lett.* **60**, 217 (1999).
28. Gandía, L. M., Malm, R., Marchand, R., Conanec, R., Laurent, Y., and Montes, M., *Appl. Catal A* **114**, L1 (1994).
29. Narayanan, S., and Unnikrishnan, *Appl. Catal A* **145**, 231 (1996).
30. Gõni, D., Melo, L., Giannetto, G., Magnoux, P., Guisnet, M., and Lavaud, N., *in* "Proceedings, XVIII Iberoamerican Symposium on Catalysis" (J. L. Figueiredo, Ed.), acibas 402-C-516. FEUP, Porto, Portugal, 2000.
31. Veloso, C. O., Monteiro, J. L. F., and Souza-Aguiar, E. F., *Stud. Surf. Sci. Catal.* **84**, 1913 (1994).
32. Anderson, J. R., "Structure of Metallic Catalysts," Academic Press, London, 1975.

33. Anderson, J. R., and Pratt, K. C., “Introduction to Characterization and Testing of Catalysts,” Academic Press, Sydney, 1985.
34. Yagi, F., Kanuka, N., Tsuji, H., Nakata, S., Kita, H., and Hattori, H., *Microporous Mater.* **9**, 229 (1997).
35. Bertsch, L., and Habgood, H. W., *J. Phys. Chem.* **67**, 1621 (1963).
36. Kirmse, A., Kärger, J., Stallmach, F., and Hunger, B., *Appl. Catal A* **188**, 241 (1999).
37. Lavaud, N., Magnoux, P., Alvarez, F., Melo, L., Giannetto, G., and Guisnet, M., *J. Mol. Catal. A* **142**, 223 (1999).
38. Bernard, J. R., *in* “Proceedings, 5th International Zeolite Conference” (L. V. C. Rees, Ed.), p. 686. Heyden, London, 1980.
39. Zhang, G., Hattori, H., and Tanabe, K., *Appl. Catal*. **40**, 183 (1988).
40. Streitwieser, A., Heathcock, C. H., and Kosower, E. M., “Introduction to Organic Chemistry,” 4th ed. McMillan, New York, 1992.
41. Barthomeuf, D., *Catal. Rev.* **38**, 521 (1996).